

CHAPTER 5

DOUBLE RELAXATIONS OF MONOSUBSTITUTED ANILINES IN BENZENE UNDER EFFECTIVE DISPERSIVE REGIONS

5.1 Introduction

The highly nonspherical molecules like mono - or di-substituted benzenes and anilines have more than one relaxation times τ ' due to presence of their flexible parts attached to the parent molecule^{1,2}. The study of dielectric relaxation phenomena of such polar molecules in nonpolar solvent provides one with the valuable information of various types of interactions such as monomer and dimer formations³⁻⁵ in liquids. The polar nonpolar liquid mixtures instead of pure polar liquids deserve much more advantages as the polar - polar interactions, viscosity effect and the other factors become minimized. Moreover, much disputed ambiguity concerning the internal field correction can also be avoided.

Bergmann *et al*⁶ however, devised a graphical method to obtain τ_1 and τ_2 to represent the relaxation times of the smallest flexible part as well as the whole molecule for their end-over-end rotations under an electric field of Giga hertz frequency. The respective contributions c_1 and c_2 towards dielectric relaxation were also estimated in terms of τ_1 and τ_2 . The method consists of plotting the normalised experimental points involved with the measured data of the real ϵ' , the imaginary ϵ'' parts of the complex dielectric constant ϵ^* , the static dielectric constant ϵ_0 and the optical dielectric constant ϵ_∞ at different frequencies ω on a semicircle in a complex plane. A point was, however, then selected on the chord through the two fixed points lying on the said semicircle which contained all the experimental points in consistency with the measured data for various frequencies. Bhattacharyya *et al*⁷ subsequently simplified the above procedure to get τ_1 , τ_2 and the weighted contributions c_1 and c_2 towards dielectric relaxations with the experimental values of ϵ' , ϵ'' , ϵ_0 and ϵ_∞ of a pure polar liquid measured at two different frequencies in GHz regions.

The highly nonspherical polar liquid molecules like mono-or di-substituted anilines and benzenes are usually thought to absorb energy much more strongly in a high frequency electric field of nearly 10 GHz. Moreover, such type of polar liquids are supposed to be non-Debye in their relaxation behaviours. From this point of view, the study of dielectric

relaxation of polar-nonpolar liquid mixtures under the electric field of nearly 3 cm wavelength is preferable. Saha *et al*¹ and Sit *et al*² recently presented an alternative approach to estimate τ_1 and τ_2 from the intercept and the slope of a derived straight line equation involved with dielectric relaxation solution data like ϵ'_{ij} , ϵ''_{ij} , ϵ_{0ij} and $\epsilon_{\infty ij}$ measured under a single frequency electric field of GHz range. One could not make a strong conclusion if ϵ_{0ij} and $\epsilon_{\infty ij}$ of a polar solute (*j*) dissolved in a nonpolar solvent (*i*) were not accurately known.

Table 5.1 The dielectric relaxation parameters like ϵ'_{ij} , ϵ''_{ij} , ϵ_{0ij} and $\epsilon_{\infty ij}$ of three isomers of anisidines and toluidines in benzene for different weight fractions ω_j 's of solutes at 35°C under effective dispersive region of 9.945 GHz electric field.

System	Weight fraction (ω_j) of solute	ϵ'_{ij}	ϵ''_{ij}	ϵ_{0ij} at 450 KHz	$\epsilon_{\infty ij} = n^2 D_{ij}$
I) o-anisidine in benzene	0.0326	2.3104	0.0148	2.336	2.239
	0.0604	2.3520	0.0244	2.404	2.247
	0.0884	2.4064	0.0340	2.459	2.255
	0.1135	2.4416	0.0400	2.538	2.262
	0.1361	2.4672	0.0512	2.588	2.267
II) m- anisidine in benzene	0.0160	2.2720	0.0234	2.315	2.235
	0.0336	2.3040	0.0390	2.384	2.241
	0.0579	2.3904	0.0618	2.477	2.246
	0.0823	2.4544	0.0744	2.553	2.253
	0.1109	2.5344	0.1056	2.675	2.261
III) p- anisidine in benzene	0.0319	2.3104	0.0252	2.373	2.237
	0.0597	2.3904	0.0474	2.442	2.246
	0.0848	2.5088	0.0642	2.539	2.250
	0.1106	2.5376	0.0840	2.638	2.262
	0.1396	2.6272	0.1086	2.745	2.269
IV) o- toluidine in benzene	0.0137	2.2752	0.0162	2.301	2.241
	0.0459	2.3648	0.0408	2.392	2.250
	0.0622	2.4032	0.0570	2.457	2.255
	0.1048	2.5376	0.0900	2.577	2.264
V) m- toluidine in benzene	0.0264	2.3136	0.0150	2.337	2.243
	0.0538	2.3552	0.0342	2.413	2.248
	0.0781	2.4576	0.0402	2.470	2.252
	0.1015	2.3840	0.0618	2.526	2.258
	0.1225	2.5280	0.0732	2.591	2.262
VI) p- toluidine in benzene	0.0213	2.3100	0.0102	2.319	2.237
	0.0428	2.3040	0.0204	2.367	2.244
	0.0616	2.3904	0.0276	2.413	2.249
	0.0916	2.4704	0.0384	2.483	2.254
	0.1048	2.4960	0.0582	2.523	2.260

Disubstituted anilines and benzenes were found to possess the double relaxation phenomena¹ by showing considerable values of τ_1 and τ_2 in solvent benzene under the electric field of 9.945 GHz. Monosubstituted anilines, however, showed mono as well as often the double relaxation phenomena² in solvent benzene under the electric field of different frequencies of 2.02 to 22.06 GHz. We, therefore, thought to use ϵ'_{ij} , ϵ''_{ij} , ϵ_{0ij} and $\epsilon_{\infty ij}$ of such monosubstituted anilines for different weight fractions ω_j 's under 9.945 GHz electric field which is supposed to be the most effective dispersive region for such isomers of anisidine and toluidine. The dielectric relaxation parameters were, however, obtained at 35°C as shown in Table 5.1 from the careful graphical interpolation made by the available data measured by Srivastava and Suresh Chandra⁸ at different frequencies.

The monosubstituted anilines are really found to exhibit the expected double relaxation phenomenon under 9.945 GHz electric field at 35°C by showing reasonable values of τ_1 and τ_2 as presented in Table 5.2, from the slopes and the intercepts of curves of Fig 5.1 as derived from Bergmann's equations. The relative contributions c_1 and c_2 (Table 5.3) towards dielectric relaxations in terms of estimated τ_1 and τ_2 (Table 5.2) were evaluated by the graphical method^{1,2} using Figs 5.2 and 5.3 as well as by Fröhlich's equations⁹ respectively. The symmetric and the asymmetric distribution parameters of such compounds under the effective dispersive region of 9.945 GHz electric field can also be judged to throw much light on their distribution behaviour (Table 5.3). In absence of the reliable τ of such isomers of anisidine and toluidine, the slope of the linear variations of the imaginary parts K''_{ij} against the real parts K'_{ij} of the complex hf conductivities K^*_{ij} of solutions were used to get τ as shown in Table 5.2, together with τ_0 , τ_s and τ_{cs} where τ_0 is the most probable relaxation time given by $\tau_0 = \sqrt{\tau_1 \tau_2}$, τ_s and τ_{cs} are called symmetric and characteristic relaxation times associated with symmetric and asymmetric distribution parameters γ and δ respectively. The respective dipole moments μ_1 , μ_2 and μ_0 in terms of τ_1 , τ_2 and τ_0 of these compounds as obtained from the slope β of the linear variations of total hf conductivities K_{ij} 's of the solutions against ω_j 's of monosubstituted anilines in

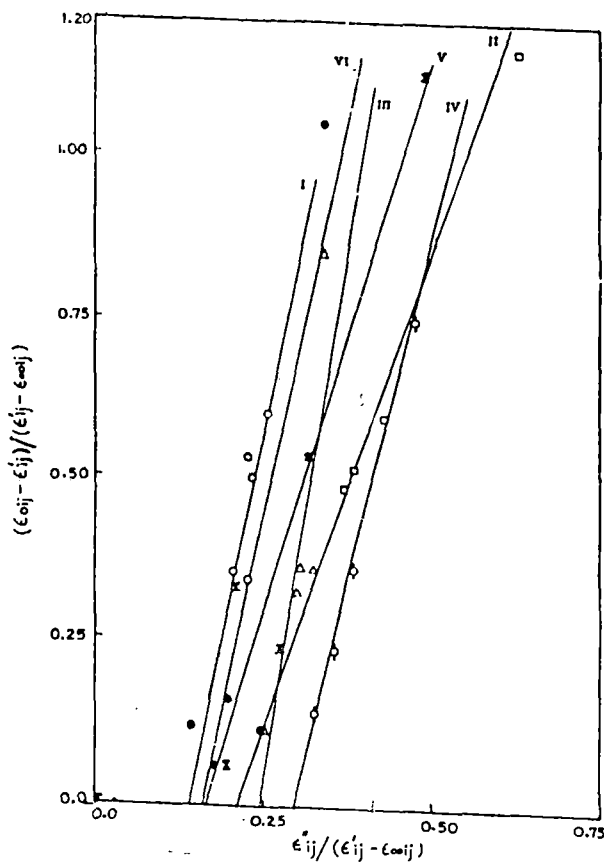


Figure 5.1 Linear variation of $(\epsilon_{0ij} - \epsilon'_{ij}) / (\epsilon'_{ij} - \epsilon_{\infty ij})$ against $\epsilon''_{ij} / (\epsilon'_{ij} - \epsilon_{\infty ij})$ of mono-substituted anilines under 9.945 GHz electric field at 35°C

System-I: *o*-anisidine (-O-) System-II: *m*-anisidine (-□-)
 System-III: *p*-anisidine (-Δ-) System-IV: *o*-toluidine (-◇-)
 System-V: *m*-toluidine (-X-) System-VI: *p*-toluidine (-●-)

Table 5.2 The slope and intercept of the straight lines of $[(\epsilon_{0ij} - \epsilon'_{ij})/(\epsilon'_{ij} - \epsilon_{\infty ij})]$ against $[(\epsilon''_{ij})/(\epsilon'_{ij} - \epsilon_{\infty ij})]$, correlation co-efficients (r), % of error involved, relaxation times τ_1 and τ_2 of the flexible parts as well as the whole molecules, measured τ from $K''_{ij} - K'_{ij}$ equations and the most probable relaxation times τ_0 together with τ_s and τ_{cs} from symmetric and asymmetric distribution parameters γ and δ of monosubstituted anilines at 35°C under 9.945 GHz electric field

System with Sl. No.	Slope and straight lines Eq(5.7) versus [$(\epsilon''_{ij})/$ $(\epsilon'_{ij} - \epsilon_{\infty ij})]$	intercept of lines Eq(5.7) $(\epsilon'_{ij} - \epsilon_{\infty ij})$	Correlation Co-efficient (r)	% of error involved in Eq (5.7)	Estimated times τ_1 p	relaxation and τ_2 in sec	Most probable relaxation time $\tau_0 = (\tau_1\tau_2)^{1/2}$	Measured τ from $K''_{ij} - K'_{ij}$ Eq (5.20) in p sec	τ_s from symmetric distribution parameter γ of Eq (5.13)	τ_{cs} from asymmetric distribution parameter δ of Eq (5.15)
I o-anisidine	4.9294	0.6583	0.7789	11.86	2.20	76.73	12.99	3.54	0.55	61.91
II m-anisidine	2.9043	0.6073	0.9888	0.67	3.63	42.87	12.47	4.77	14.78	86.39
III p-anisidine	6.2098	1.4923	0.8308	9.34	4.01	95.42	19.56	4.20	1.41	75.33
IV o-toluidine	4.2660	1.2707	0.9994	0.04	5.16	63.15	18.05	4.56	4.62	41.71
V m-toluidine	3.3514	0.5415	0.9622	2.24	2.73	50.94	11.79	5.52	0.64	66.69
VI p-toluidine	4.7133	0.7348	0.8684	7.41	2.58	72.88	13.71	3.57	0.66	20.13

Table 5.3 The estimated values of $x [= (\epsilon'_{ij} - \epsilon_{\infty ij}) / (\epsilon_{0ij} - \epsilon_{\infty ij})]$ and $y [= \epsilon''_{ij} / (\epsilon_{0ij} - \epsilon_{\infty ij})]$ from Fröhlich's equations and by the graphical techniques at $\omega_j \rightarrow 0$. Fröhlich's parameter A, symmetric and asymmetric distribution parameters γ and δ from x and y at $\omega_j \rightarrow 0$ along with the relative contributions c_1 and c_2 due to Fröhlich and the graphical technique under 9.945 GHz electric field

System with SI No.	Fröhlich's parameter $A = \ln(\tau_1 / \tau_2)$	Estimated x and y from Eq (5.8) & (5.9)	values of Fröhlich's (5.9)	Weighted c_1 & c_2 Eq (5.5) & (5.6)	contribution from (5.6)	Estimated x & y from Fig at $\omega_j \rightarrow 0$	values of (5.2) & (5.3)	Weighted c_1 & c_2 graphical	contributions from the technique	Symmetric & distribution γ & δ	asymmetric parameters
I o-anisidine	3.5518	0.5555	0.3457	0.5069	1.3869	0.0875	0.106	0.8946	-0.0732	0.47	0.09
II m-anisidine	2.4689	0.5848	0.4009	0.4997	0.8945	0.515	0.254	0.4825	0.4574	0.40	0.33
III p-anisidine	3.1695	0.4420	0.3655	0.4223	1.6298	0.810	0.140	0.8725	-0.4020	0.49	0.13
IV o-toluidine	2.5046	0.4594	0.4033	0.4293	1.1669	0.740	0.228	1.1326	-0.0478	0.35	0.25
V m-toluidine	2.9263	0.5933	0.3748	0.5170	1.0107	0.870	0.106	0.9097	-0.1564	0.49	0.09
VI p-toluidine	3.3410	0.5432	0.3574	0.4942	1.3351	0.950	0.084	0.9908	-0.3417	0.29	0.09

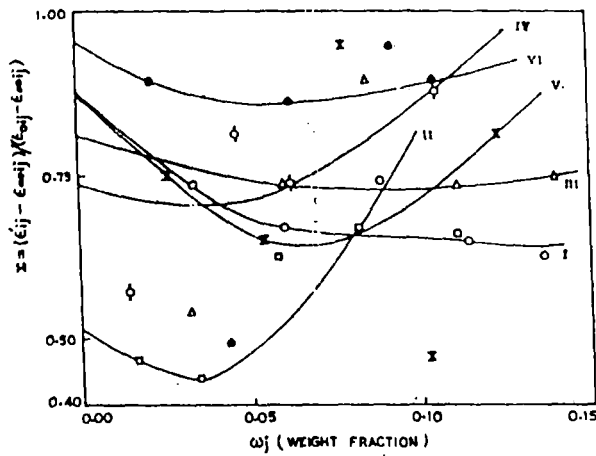


Figure 5.2 Variation of $(\epsilon'_{ij} - \epsilon_{\infty ij}) / (\epsilon_{0ij} - \epsilon_{\infty ij})$ against weight fraction ω_j ' of solutes under 9.945 GHz electric field at 35°C
 System-I: *o*-anisidine (-O-) System-II: *m*-anisidine (-□-)
 System-III: *p*-anisidine (-Δ-) System-IV: *o*-toluidine (-◇-)
 System-V: *m*-toluidine (-X-) System-VI: *p*-toluidine (-●-)

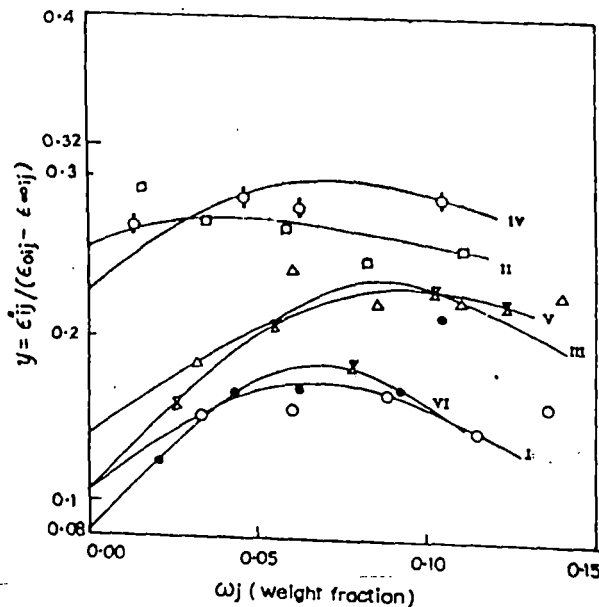


Figure 5.3 Variation of $\epsilon''_{ij} / (\epsilon'_{ij} - \epsilon_{\infty ij})$ against ω_j ' of isomers of anisidines and toluidines under 9.945 GHz electric field at 35°C
 System-I: *o*-anisidine (-O-) System-II: *m*-anisidine (-□-)
 System-III: *p*-anisidine (-Δ-) System-IV: *o*-toluidine (-◇-)
 System-V: *m*-toluidine (-X-) System-VI: *p*-toluidine (-●-)

benzene (Fig 5.4) are in close agreement with the theoretical dipole moments μ_{theo} (Table 5.4) as computed from bond angles and bond moments of several groups in anisidines and toluidines with respect to benzene ring.

5.2 Theory and Formulation

When the polar molecule is provided with more than one relaxation times i. e., τ_1 and τ_2 Debye's equations of polar - nonpolar liquid mixture lead to Bergmann's equations :

$$\frac{\epsilon'_{ij} - \epsilon_{\infty ij}}{\epsilon_{0ij} - \epsilon_{\infty ij}} = \frac{c_1}{1 + \omega^2 \tau_1^2} + \frac{c_2}{1 + \omega^2 \tau_2^2} \quad \dots\dots(5.1)$$

$$\frac{\epsilon''_{ij}}{\epsilon_{0ij} - \epsilon_{\infty ij}} = c_1 \frac{\omega \tau_1}{1 + \omega^2 \tau_1^2} + c_2 \frac{\omega \tau_2}{1 + \omega^2 \tau_2^2} \quad \dots\dots(5.2)$$

such that $c_1 + c_2 = 1$.

The co-efficients c_1 and c_2 are the weight factors of the two Debye processes governed by τ_1 and τ_2 respectively. The symbols used in Eqs (5.1) and (5.2) convey the usual meanings:

$$\text{Let } x = \frac{\epsilon'_{ij} - \epsilon_{\infty ij}}{\epsilon_{0ij} - \epsilon_{\infty ij}}, \quad y = \frac{\epsilon''_{ij}}{\epsilon_{0ij} - \epsilon_{\infty ij}}$$

and $\omega\tau = \alpha$. Using the notations $a = 1/(1+\alpha^2)$ and $b = \alpha/(1+\alpha^2)$ the above Eqs (5.1) and (5.2) can be written as :

$$x = c_1 a_1 + c_2 a_2 \quad \dots\dots(5.3)$$

$$y = c_1 b_1 + c_2 b_2 \quad \dots\dots(5.4)$$

The suffices 1 and 2 with a and b are related to τ_1 and τ_2 respectively.

Evaluating c_1 and c_2 from Eqs (5.3) and (5.4) one gets:

Table 5.4 Intercepts and slope of $K_{ij}-\omega_j$ curve, dimensionless parameters b_0, b_1, b_2 dipole moments μ_1, μ_2 in Debye (D) together with estimated μ_1 from $\mu_1 = \mu_2 (c_1/c_2)^{1/2}$ and theoretical μ from bond angles and bond moments of isomers of anisidine and toluidine at 9.945 GHz electric field at 35°C

System with Sl.No. & mol wt	Intercept & slope of $K_{ij}-\omega_j$ equation		Dimensionless parameter			Estimated dipole moments in Debye			μ_{theo} in D from bond angles and bond moments	Estimated μ_1 from $\mu_1 =$ $\mu_2 (c_1/c_2)^{1/2}$ in D
	$\alpha \times 10^{-10}$ esu	$\beta \times 10^{-10}$ esu	$b_0 =$ $\frac{1}{1 + \omega^2 \tau_0^2}$	$b_1 =$ $\frac{1}{1 + \omega^2 \tau_1^2}$	$b_2 =$ $\frac{1}{1 + \omega^2 \tau_2^2}$	μ_0 D	μ_1 D	μ_2 D		
I o-anisidine $M_j = 123$ gm	1.1244	0.7757	0.6030	0.9815	0.0417	2.45	1.92	9.33	1.02	5.64
II m-anisidine $M_j = 123$ gm	1.1039	1.4215	0.6224	0.9511	0.1224	3.27	2.264	7.37	1.65	5.51
III p-anisidine $M_j = 123$ gm	1.1060	1.4663	0.4012	0.9410	0.0274	4.13	2.70	15.82	1.89	8.05
IV o-toluidine $M_j = 107$ gm	1.1151	1.1932	0.4404	0.9059	0.0604	3.32	2.31	8.96	1.39	5.43
V m-toluidine $M_j = 107$ gm	1.1359	0.5788	0.6484	0.9718	0.0899	1.91	1.56	5.12	1.03	3.66
VI p-toluidine $M_j = 107$ gm	1.1323	0.3501	0.5770	0.9747	0.0460	1.57	1.21	5.56	1.54	3.38

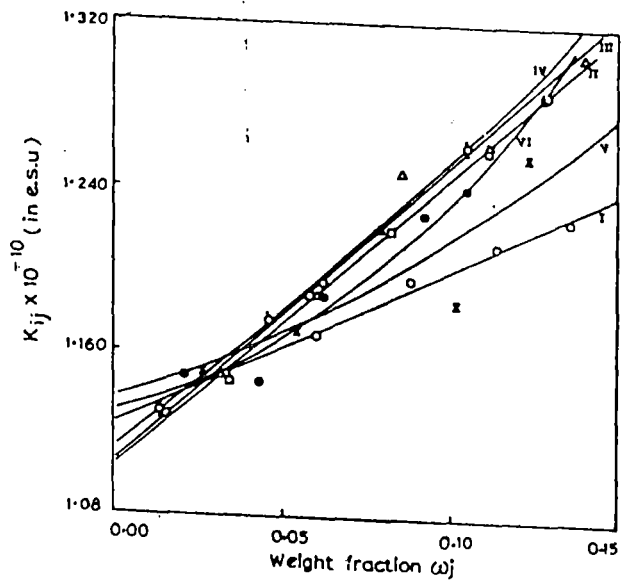


Figure 5.4 Variation of hf conductivity K_{ij} with different weight fractions ω_j ' of solutes at 35°C and 9.945 GHz electric field
 System-I: *o*-anisidine (-O-) System-II: *m*-anisidine (-□-) System-III: *p*-anisidine (-Δ-) System-IV: *o*-toluidine (-⊙-) System-V: *m*-toluidine (-X-) System-VI: *p*-toluidine (-●-)

$$c_1 = \frac{(x\alpha_2 - y)(1 + \alpha_1^2)}{\alpha_2 - \alpha_1} \quad \dots\dots\dots(5.5)$$

and

$$c_2 = \frac{(y - x\alpha_1)(1 + \alpha_2^2)}{\alpha_2 - \alpha_1} \quad \dots\dots\dots(5.6)$$

provided $\alpha_2 > \alpha_1$. Now adding Eqs (5.5) and (5.6) and since $c_1 + c_2 = 1$ we get :

$$\frac{1-x}{y} = (\alpha_1 + \alpha_2) - \frac{x}{y} \alpha_1 \alpha_2$$

which on substitution of the values of x, y and α yields :

$$\frac{\epsilon_{0ij} - \epsilon'_{ij}}{\epsilon'_{ij} - \epsilon_{\infty ij}} = \omega (\tau_1 + \tau_2) \frac{\epsilon''_{ij}}{\epsilon'_{ij} - \epsilon_{\infty ij}} - \omega^2 \tau_1 \tau_2 \quad \dots\dots\dots(5.7)$$

representing a straight line of $[(\epsilon_{0ij} - \epsilon'_{ij})/(\epsilon'_{ij} - \epsilon_{\infty ij})]$ against $[\epsilon''_{ij}/(\epsilon'_{ij} - \epsilon_{\infty ij})]$ with slope $\omega(\tau_1 + \tau_2)$ and intercept $-\omega^2 \tau_1 \tau_2$. The slopes and intercepts of Eq. (5.7) were, however, evaluated by fitting ϵ'_{ij} , ϵ''_{ij} , ϵ_{0ij} and $\epsilon_{\infty ij}$ for different ω 's of the monosubstituted anilines. referred to Tables (5.1-5.4) and Figs (5.1-5.4) at 35°C under 9.945 GHz electric field. They are finally placed in Table 5.2. to yield, τ_1 and τ_2 respectively for them.

The weighted contributions c_1 and c_2 towards dielectric relaxation may be computed from Eqs (5.5) and (5.6) using x and y in Fröhlich's equations⁹

$$x = \frac{\epsilon'_{ij} - \epsilon_{\infty ij}}{\epsilon_{0ij} - \epsilon_{\infty ij}} = 1 - \frac{1}{2A} \ln \left(\frac{1 + e^{2A \omega^2 \tau_s^2}}{1 + \omega^2 \tau_s^2} \right) \quad \dots\dots\dots(5.8)$$

and

$$y = \frac{\epsilon''_{ij}}{\epsilon_{0ij} - \epsilon_{\infty ij}} = \frac{1}{A} [\tan^{-1}(e^{A \omega \tau_s}) - \tan^{-1}(\omega \tau_s)] \quad \dots\dots\dots(5.9)$$

where A = Fröhlich parameter = $\ln(\tau_2/\tau_1)$ and τ_s = small limiting relaxation time = τ_1 . Both c_1 and c_2 may also be calculated from Eqs (5.5) and (5.6) with the graphically extrapolated

fixed values of x and y when $\omega_j \rightarrow 0$ as shown in Figs (5.2) and (5.3). They are shown in Table 5.3.

The molecules appear to behave like nonrigid ones having either symmetric or asymmetric distribution parameters γ and δ which may be calculated from Eqs (5.10-5.11)

$$\epsilon_{ij}^* = \epsilon_{\infty ij} + \frac{\epsilon_{0ij} - \epsilon_{\infty ij}}{1 + (j\omega\tau_s)^2} \quad \dots\dots(5.10)$$

or,

$$\epsilon_{ij}^* = \epsilon_{\infty ij} + \frac{\epsilon_{0ij} - \epsilon_{\infty ij}}{(1 + j\omega\tau_{cs})^2} \delta \quad \dots\dots (5.11)$$

where $j = \sqrt{-1}$.

The former and the latter ones are associated with τ_s and τ_{cs} where τ_s and τ_{cs} are called the symmetric as well as the characteristic relaxation times. Separating the real and the imaginary parts of Eqs (5.10) and (5.11) and rearranging them in terms of x and y as shown in Figs (5.3) and (5.4) at $\omega_j \rightarrow 0$ we have the symmetric parameter γ from :

$$\gamma = \frac{2}{\pi} \tan^{-1} \left[(1-x) \frac{x}{y} - y \right] \quad \dots\dots(5.12)$$

$$\tau_s = \frac{1}{\omega} \left\{ \frac{1}{\left[\begin{array}{c} x \\ y \end{array} \cos \left(\frac{\gamma\pi}{2} \right) - \sin \left(\frac{\gamma\pi}{2} \right) \right]} \right\}^{1/(1-\gamma)} \quad \dots\dots(5.13)$$

similarly, δ and τ_{cs} can be had from Eqs (5.11) as:

$$\tan^{-1}(\delta\phi) = \frac{y}{x} \quad \dots\dots(5.14)$$

and

$$\tan \phi = \omega\tau_{cs} \quad \dots\dots (5.15)$$

As the values of ϕ can not be estimated directly we draw a theoretical curve for $\log (\cos\phi)^{1/\phi}$ against ϕ as shown in Fig 5.5 from which.

$$\log (\cos \phi) \cdot 1/\phi = \frac{\log \frac{x}{\cos (\delta \phi)}}{\delta \phi} \quad \text{.....(5.16)}$$

can be known. With the known ϕ from Fig 5.5 ; τ_{es} and δ can be estimated from Eqs (5.14) and (5.15) respectively. The τ_s and τ_{es} thus estimated are placed in Table 5.2 to compare with τ_1 and τ_2 from double relaxation method, but γ and δ are placed in Table 5.3

The complex high frequency conductivity K_{ij}^* of a dilute polar - nonpolar liquid mixture¹² is given by :

$$K_{ij}^* = K'_{ij} + jK''_{ij} \quad \text{.....(5.17)}$$

$$\text{where } K'_{ij} = \frac{\omega}{4\pi} \epsilon''_{ij} \text{ and } K''_{ij} = \frac{\omega}{4\pi} \epsilon'_{ij}$$

The magnitude of the total hf conductivity is :

$$K_{ij} = \frac{\omega}{4\pi} (\epsilon''_{ij}{}^2 + \epsilon'_{ij}{}^2)^{\frac{1}{2}} \quad \text{.....(5.18)}$$

The dielectric permittivity ϵ'_{ij} of solution in hf region is very small and eventually equals the optical dielectric constant. The dielectric loss ϵ''_{ij} is responsible for the absorption of electrical energy and, therefore, offers resistance to polarisation. The K_{ij} may thus be approximated as :

$$K_{ij} = \frac{\omega}{4\pi} \epsilon''_{ij} \text{ since } \epsilon''_{ij} \gg \epsilon'_{ij}$$

The real part of the complex conductivity of a solution of weight - fraction ω_j of polar solute at T K is :

$$K'_{ij} = \frac{\mu_j^2 N \rho_{ij} F_{ij}}{3M_j kT} \left(\frac{\omega^2 \tau}{1 + \omega^2 \tau^2} \right) \omega_j \quad \text{.....(5.19)}$$

where the symbols have their usual significance. But for hf region it can be shown that

$$K''_{ij} = K_{\infty ij} + \frac{K'_{ij}}{\omega \tau}$$

$$\text{or, } K_{ij} = K_{\infty ij} + \frac{K'_{ij}}{\omega \tau} \quad \text{.....(5.20)}$$

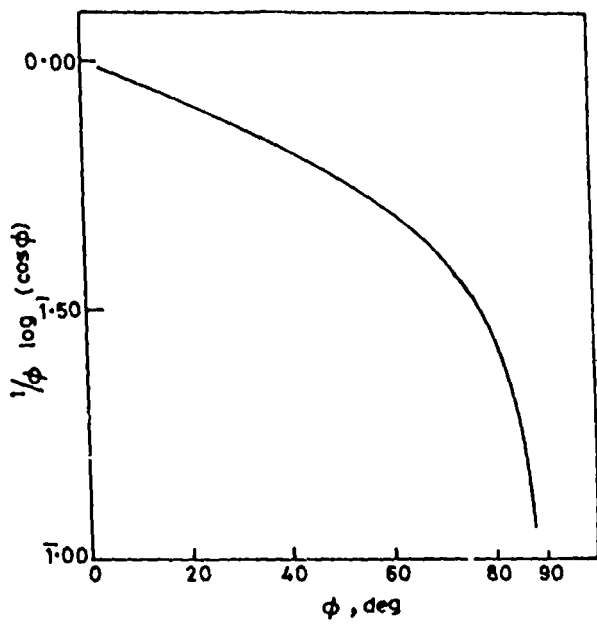


Figure 5.5 Variation of $\log(\cos \phi)^{1/\phi}$ against ϕ

Since K_{ij} is a function of ω_j , it can be shown at infinite dilution :

$$\left(\frac{dK'_{ij}}{d\omega_j} \right)_{\omega_j \rightarrow 0} = \omega \tau \beta \quad \dots\dots(5.21)$$

where β is the slope of $K_{ij} - \omega_j$ curve at $\omega_j \rightarrow 0$. Eq (5.19) on being differentiated with respect to ω_j and at $\omega_j \rightarrow 0$ becomes.

$$\left(\frac{dK'_{ij}}{d\omega_j} \right)_{\omega_j \rightarrow 0} = \frac{\mu_j^2 N \rho_i F_i}{3 M_j kT} \left(\frac{\omega^2 \tau}{1 + \omega^2 \tau^2} \right) \quad \dots\dots(5.22)$$

because at $\omega_j \rightarrow 0$, ρ_{ij} the density of the solution becomes ρ_i , the density of the solvent and F_{ij} the local field in the solution becomes F_i , where $F_i = [(\epsilon_i + 2)/3]^2$, ϵ_i , is the dielectric constant of the solvent. From Eqs. (5.21) and (5.22) we finally get :

$$\mu_j = \left(\frac{3 M_j kT \beta}{N \rho_i F_i \omega b} \right)^{1/2} \quad \dots\dots(5.23)$$

as the dipole moment of the polar liquid in terms of b where

$$b = \frac{1}{1 + \omega^2 \tau^2} \quad \dots\dots(5.24)$$

which is a dimensionless parameter. The μ_1 , μ_2 and μ_0 in terms of b_1 , b_2 and b_0 involved with τ_1 , τ_2 and τ_0 respectively were then computed with the knowledge of β . They are finally placed in Table 5.4 together with μ_{theo} obtained from bond angles and bond moments for comparison.

5.3 Results and Discussion

The values of x and y in terms of dielectric relaxation data at 9.945 GHz as shown in Table 5.1 are first estimated for different ω_j 's with the available data⁸ measured under 2.02, 3.86 and 22.06 GHz electric field. They are then plotted against ω_j 's as shown in Figs (5.2) and (5.3) which are found to agree well with the Bergmann Eqs (5.1) and (5.2)

almost exactly. The close agreement of the curves in Figs (5.2) and (5.3), with Eqs. (5.1) and (5.2) suggests that the data (Table (5.1)) selected by graphical interpolations at 3 cm wavelength electric field are almost accurate. The dielectric relaxation parameters ϵ'_{ij} , ϵ''_{ij} , ϵ_{0ij} , and $\epsilon_{\infty ij}$ thus obtained, are used to calculate the slopes and the intercepts of the fitted straight lines of Eq. (5.7) with the experimental points placed upon them as shown in Fig 5.1. The correlation coefficient r for each straight line is, however, estimated and found to lie within the range of 0.9994 to 0.7789 together with % error involved in each case. They are shown in 4th and 5th columns of Table 5.2. Table 5.2 also shows that *o*- and *p*-anisidine like *p*-toluidine exhibit errors of larger magnitudes than the other systems. This may, perhaps, be due to the uncertainty in the estimation of dielectric relaxation data for such systems. Monosubstituted anilines often showed double as well as mono relaxation behaviour as observed earlier². *p*-anisidine, however, is an exception². It showed the mono relaxation behaviour at 2.02, 3.86 and 22.06 GHz respectively. It is again very much interesting to note that all the anisidines and toluidines as referred to Table 5.2, nevertheless exhibit the double relaxation behaviour by showing reasonably considerable values of τ_1 (smaller) and τ_2 (larger) to represent the relaxation times for their flexible parts attached to the parent ring and the whole molecules respectively. It signifies that 9.945 GHz (\cong 3 cm wavelength) electric field seems to be the most effective dispersive region for such molecule to yield τ_1 and τ_2 .

The τ_2 's as observed from the slopes and the intercepts of Eq. (5.7) gradually increase from *meta*- to *ortho*- and to *para*-forms of all the anisidines and toluidines probably due to C—NH₂ groups which is highly influenced by 9.945 GHz (\cong 3 cm wavelength) electric field for its different positions in them. The τ_1 's, on the other hand, increase from *ortho* to *para* for anisidines while reverse is true for toluidines. The increase in the values of τ_1 's indicates the flexible parts of the molecules are more loosely bound to parent molecules^{1,2}.

The most probable relaxation time τ_0 as shown in the 8th column of Table 5.2, can be compared with the measured τ 's from the slopes⁵ of K''_{ij} - K'_{ij} along with symmetric τ_s and characteristic τ_{cs} from γ and δ . The τ 's as shown in the 9th column of Table 5.2 agree

excellently well with τ_1 . This fact indicates that the *hf* conductivity measurement of polar - nonpolar liquid mixture yields the microscopic relaxation time while the double relaxation method gives macroscopic as well as microscopic relaxation times as observed earlier¹³. τ_{cs} ' in Table 5.2 are slightly smaller than τ_s ', as obtained from *hf* conductivity for almost all systems besides *m*-ianisidine and *o*-toluidine whose τ_{cs} ' agree well with τ_0 and τ respectively. The slight difference is due to different steric hindrances as a result of structural conformations. All these discussions made above, confirms τ_s to represent microscopic relaxation time. τ_{cs} 's, on the other hand, are larger in magnitude and agree with τ_2 as obtained by double relaxation method. Thus τ_{cs} under the electric field of 9.945 GHz gives τ_2 .

The relative contributions c_1 and c_2 towards dielectric relaxations were found out in the graphical method by using Figs 5.2 and 5.3 as well as Fröhlich's equations of

$$x = \left[\frac{\epsilon'_{ij} - \epsilon_{\infty ij}}{\epsilon_{0ij} - \epsilon_{\infty ij}} \right] \quad \text{and} \quad y = \left[\frac{\epsilon''_{ij}}{\epsilon_{0ij} - \epsilon_{\infty ij}} \right] \quad \text{both from Bergmann's Eqs (5.1) and (5.2) in}$$

terms of τ_1 and τ_2 . The x and y in Fröhlich's Eqs (5.8) and (5.9) are related to Fröhlich parameter A which depends on the difference of the activation energies E_2 and E_1 of the rotating units and is expressed in terms of τ_2/τ_1 by $\tau_2/\tau_1 = \exp(E_2 - E_1)/RT$. The constancy of the factor $(E_2 - E_1)/RT$ at a fixed temperature may be put equal to A where $A = \ln(\tau_2/\tau_1)$. The positive values of c_1 and c_2 such that $c_2 > c_1$ and $c_1 + c_2 > 1$ in Fröhlich's method for all the systems are shown in the 5th and 6th columns of Table 5.3 together with the Fröhlich parameters A in the 2nd column respectively. But the graphical extrapolation technique suggested by Saha *et al*¹ and Sit *et al*², however, yields c_2 always negative except *m*-anisidine satisfying the condition that $c_1 + c_2 \cong 1$ as shown in the 9th and 10th columns of same Table 5.3. The negative sign before c_2 in the latter method signifies the lag in inertia of the whole molecules with respect to their flexible parts^{1,2} under *hf* electric field.

The double relaxation times showed by all the monosubstituted anilines under 9.945 GHz electric field at 35°C indicate the nonrigidity of the molecules. This fact at once inspired us to test the symmetric as well as asymmetric distribution parameters γ and δ for

such compounds. They are calculated from Eqs (5.12) and (5.16) with the values of x and y at $\omega_j \rightarrow 0$ from Figs 5.2 and 5.3. The values of γ and δ thus obtained with the aid of the direct measurements of relaxation data seem to be accurate enough to specify the distribution parameters as placed in the last two columns of Table 5.3. It is observed from Table 5.3 that the values of γ lie in the range of $0.29 \leq \gamma \leq 0.49$ indicating thereby symmetric relaxation behaviour for such molecules under 9.945 GHz electric field. The low values of δ in the range of $0.09 \leq \delta \leq 0.33$ invariably rules out the possibility of occurrence of asymmetric dielectric distributions¹⁴.

The dipole moments μ_1 and μ_2 of the flexible parts and the whole molecules of anisidines and toluidines are obtained from Eq. (5.23) in terms of dimensionless parameters b_1, b_2 from Eq. (5.24) involved with τ_1 and τ_2 respectively (Table 5.2) and the slope β of $K_{ij} - \omega_j$ curves in Fig 5.4 which shows the variation of $K_{ij}s'$ with $\omega_j s'$. The intercepts and slopes of $K_{ij} - \omega_j$ equations are shown in the 2nd and 3rd columns of Table 5.4. The intercepts are of almost equal in magnitudes in all of them, but the slopes β increase slowly from *ortho*-to *para*- for anisidines and reverse in toluidines. The almost same intercepts and slopes of $K_{ij} - \omega_j$ curves in Fig 5.4 arise probably due to the identical polarity³ of the molecules. Some of the curves in Fig 5.4 meet at a point near $\omega_j \rightarrow 0$ indicating thereby solute - solvent (monomer) or solute - solute (dimer) associations in the region $0.02 < \omega_j < 0.035$ of the concentration. Unlike toluidines the most probable dipole moments μ_0 and μ_1 gradually increase from *o*- to *p*- for anisidines as reported in 7th and 8th columns of Table 5.4. μ_2s' , on the other hand, increase gradually from *m*- to *o*- with a high value in *p*- anisidine while in case of toluidines μ_2s' increase from *m*- to *p*- and *o*- configurations. The above facts, however, reveal that μ_0 as obtained from $\tau_0 = \sqrt{\tau_1 \tau_2}$ depends solely upon the group moments like μ_1 of their flexible parts. The gradual increase of μ_0 from *o*- to *p*-anisidine and from *p*- to *o*-toluidine like μ_1 is probably due to their almost same polarity as supported by the slopes $\beta s'$ of K_{ij} as a function of $\omega_j s'$ (Fig 5.4).

The theoretical dipole moments $\mu_{theo}s'$ from the bond angles and bond moments of $C \rightarrow OCH_3$ in anisidines and $C \leftarrow CH_3$ in toluidines with $C \rightarrow NH_2$ with respect to the

benzene ring were already calculated elsewhere² and placed in the 10th column of Table 5.4. They are compared with all the μ_s ' together with μ_1 from $\mu_1 = \mu_2 (c_1/c_2)^{1/2}$ assuming the two relaxation processes are equally probable.

5.4 Conclusion

The correlation coefficients r_s and hence the % of errors introduced in Eq. (5.7) with the dielectric relaxation parameters like ϵ'_{ij} , ϵ''_{ij} , ϵ_{0ij} and $\epsilon_{\infty ij}$ of the polar - nonpolar liquid mixtures under 9.945 GHz electric field at 35°C (Table 5.1) as presented in Table 5.2, are within such range that τ_1 and τ_2 as obtained from the intercepts and slopes of Eq. (5.7) are of considerable accuracy because τ_s are usually claimed to be accurate within $\pm 10\%$. The methodology of single frequency measurements of dielectric relaxation data at different ω_s seems to be much simple in comparison to the existing methods where data of pure polar liquid at two or more electric field frequencies of GHz region are, usually required. The relative contributions c_1 and c_2 in terms of τ_1 and τ_2 are, however, obtained by using Fröhlich's equations as well as graphical technique which also offers a convenient method to decide either symmetric or asymmetric distribution behaviour under the electric field of given frequency. The dipole moments μ_1 , μ_2 in terms of τ_1 and τ_2 and slope β of concentration variation of K_{ij} of polar - nonpolar liquid mixture provide the valuable information of the conformation of a complex polar liquid.

References

- 1 Saha U, Sit S. K, Basak R. C and Acharyya S, J Phys D, **27** (1994) 596.
- 2 Sit S. K; Basak R. C, Saha U and Acharyya S, J Phys D. **27** (1994) 2194.
- 3 Chatterjee A. K, Saha U, Nandi N, Basak R. C and Acharyya S, Indian J Phys **B**, **66** (1992) 291.
- 4 Saha U and Acharyya S. Indian J Pure and Appl Phys, **31** (1993) 181.
- 5 Saha U and Acharyya S. Indian J Pure and Appl Phys, **32** (1994) 346.
- 6 Bergmann K, Roberti D. M and Smyth C. P, J Phys Chem, **64** (1960) 665.

- 7 Bhattacharyya J, Hasan A, Roy S. B and Kastha G. S, J Phys Soc Japan, **28** (1970) 204.
- 8 Srivastava S. C. and Suresh Chandra, Indian J Pure and Appl Phys, **13** (1975) 101.
- 9 Fröhlich H, Theory of Dielectrics (Oxford University Press, Oxford). 1949, p 94.
- 10 Cole K. S and Cole R. H, J Chem Phys, **9** (1941) 341.
- 11 Davidson D. W and Cole R. H, J Chem Phys, **19** (1951) 1484.
- 12 Murphy F. J and Morgan S. O, Bull syst Techn J, **18** (1939) 502.
- 13 Sit S. K and Acharyya S, Indian J Phys **B**, **70** (1996) 19.
- 14 Suresh Chandra and Jai Prakash, J Phys Soc Japan, **35** (1975) 876.